general. Furthermore, the Min strain has permitted the identification of unlinked modifier loci in the mouse genome that decrease the number of intestinal adenomas arising in Min mice (*18*). Identification and characterization of potential human counterparts of these modifier loci could be useful in understanding why some FAP patients develop many fewer tumors than average (*19*) and in understanding colon cancer risk in the general population.

REFERENCES AND NOTES

1. P. G. Ashton-Rickardt *et al.*, *Oncogene* **4**, 1169 (1989); P. Delattre *et al.*, *Lancet* ii, 353 (1989); D. J. Law *et al.*, *Science* **241**, 961 (1988); M. Sasaki *et al.*, *Cancer Res.* **49**, 4402 (1989); W. F. Bodmer *et al.*, *Nature* **328**, 614 (1987); M. Leppert *et al.*, *Science* **238**, 1411 (1987); P. Meera Khan *et al.*, *Hum. Genet.* **79**, 183 (1988); Y. Nakamura *et al.*, *Am. J. Hum. Genet.* **43**, 638 (1988); B. Vogelstein *et al.*, *N. Engl. J. Med.* **319**, 525 (1988); B. Vogelstein *et al.*, *Science* **244**, 207 (1989); E. Solomon *et al.*, *Nature* **328**, 616 (1987).
2. K. W. Kinzler *et al.*, *Science* **251**, 1366 (1991).
3. K. W. Kinzler *et al.*, *ibid.* **253**, 661 (1991).
4. G. Joslyn *et al.*, *Cell* **66**, 601 (1991).
5. I. Nishisho *et al.*, *Science* **253**, 665 (1991).
6. J. Groden *et al.*, *Cell* **66**, 589 (1991).
7. E. J. Gardner and R. C. Richards, *Am. J. Hum. Genet.* **5**, 139 (1953); S. Bulow, in *Familial Adenomatous Polyposis*, L. Herrera, Ed. (Liss, New York, 1990), p. 109; D. G. Jagelman, *Cancer Genet. Cytogenet.* **27**, 319 (1987).
8. A. R. Moser *et al.*, *Science* **247**, 322 (1990).
9. Human cDNA fragments of the APC gene corresponding to nucleotides 664 to 2267 and 2517 to 3183 were used in the first round screening. Fragments 3161 to 5383 and 5762 to 7430 were used in the second round screening. Fragments −22 to 659 and 6807 to 8481 were used in the third round screening. Hybridizations were carried out at 50°C in 0.5% nonfat dried milk, 1% SDS, 6% polyethylene glycol (average molecular weight 8000), 10% formamide, salmon sperm DNA (0.2 mg/ml), 0.9 M NaCl, 0.5 mM EDTA, and 0.05 M sodium phosphate (pH 7.0). Washes were performed at 55°C in 45 mM NaCl, 1.8 mM sodium citrate, 0.1 mM tris, pH 7.2, 0.1% SDS.
10. Analysis of 22 independent clones enabled us to obtain a murine sequence corresponding to 95% of the coding region of human APC (GenBank, accession no. M74088) (*3*).
11. C. Rowlatt, L. M. Franks, M. U. Sheriff, F. C. Chesterman, *J. Natl. Cancer Inst.* **43**, 1353 (1969).
12. Fifteen primer pairs for PCR and 45 internal sequencing primers were designed from the nucleotide sequence of *mApc* cDNA clones. Sequences and corresponding positions of these primers are available on request.
13. PCR products were cloned into a Bluescript vector modified [as described by T. A. Holton and M. W. Graham, *Nucleic Acids Res.* **19**, 1156 (1991)]. Pools consisting of at least 100 clones were sequenced as described by J. M. Nigro *et al.* [*Nature* **342**, 705 (1989)].
14. The nucleotide sequence of the B6 allele and the polymorphic changes in the CAST allele have been deposited in GenBank, accession no. M88127.
15. L.-K. Su *et al.*, unpublished data.
16. The A of the proposed translation initiation codon was designated nucleotide 1.
17. A combination of linkage analysis and allele-specific hybridization identified four additional mice from the AKR backcross that lacked the Min-specific mutation but did have intestinal tumors. Each of these animals had an increased life-span relative to most Min mice and had only 1 or 2 duodenal tumors. These results show that sporadic tumors occurred in mice from the AKR backcross. A similar analysis of mice from the CAST backcross yielded no evidence for sporadic tumors.
18. A. R. Moser *et al.*, *J. Cell Biol.* **116**, 1517 (1992).
19. M. Leppert *et al.*, *N. Engl. J. Med.* **322**, 904 (1990).

20. Supported in part by grants from the Clayton Fund, McAshan Fund, National Foundation for Cancer Research, Damon Runyon–Walter Winchell Cancer Fund (DRG-1058), and NIH grants CA-07175, CA-06973, CA-23076, CA-50585, and CA-35494. We thank M. Woch for care of the mouse genetic resource, E. Mattes for help with mice and with DNA preparations, N. Borenstein for numerous DNA preparations, and I. Riegel for help with the manuscript. This is publication #3230 from the Laboratory of Genetics.

30 December 1991; accepted 10 March 1992

Enhanced Degradation of the Ferritin Repressor Protein During Induction of Ferritin Messenger RNA Translation

Lisa Smith Goessling, Susan Daniels-McQueen, Maitrayee Bhattacharyya-Pakrasi, Jih-Jing Lin, Robert E. Thach*

Induction of ferritin synthesis in cultured cells by heme or iron is accompanied by degradation of the ferritin repressor protein (FRP). Intermediates in the degradative pathway apparently include FRP covalently linked in larger aggregates. The effect of iron on FRP degradation is enhanced by porphyrin precursors but is decreased by inhibitors of porphyrin synthesis, which implies that heme is an active agent. These results suggest that translational induction in this system may be caused by enhanced repressor degradation. While unique among translational regulatory systems, this process is common to a variety of other biosynthetic control mechanisms.

Synthesis of ferritin, the ubiquitous iron storage protein, is regulated at the translational level by iron in vertebrates (*1*, *2*). The regulatory machinery consists of a conserved 28-nucleotide sequence in the 5′ untranslated region of the ferritin mRNA [the iron-responsive element (IRE)] and a 98-kD protein that binds to the IRE in the absence of iron and inhibits translation. This protein is known as the ferritin repressor protein, FRP, the IRE-binding protein, or the iron regulatory factor. The FRP is a member of a family of proteins, some or all of which recognize the IRE in ferritin, transferrin (Tf) receptor, and erythroid δ-aminolevulinic acid (ALA)–synthase mRNAs (*3*–*8*). A third component of the machinery is the "inducer," which is iron complexed either with porphyrin (as heme) or with other compounds (*9*–*11*). We tested the effects of various iron sources on the turnover of FRP in cells grown in culture. Our results show that FRP normally turns over at a slow rate in vivo, but that iron, probably acting through heme, enhances the rate of FRP degradation. This effect was observed with concentrations of iron or heme that induce ferritin synthesis, which suggests that repressor degradation may be a direct cause of translational induction.

The first indication that the natural turnover of FRP might result in derepression of ferritin synthesis came from the observation that actinomycin D causes a gradual derepression of ferritin synthesis: after 19 hours of treatment, ferritin synthesis in transformed mouse cells is derepressed to approximately half the rate achieved in the presence of iron (*12*). Synthesis of no other protein is increased by actinomycin D (*13*). Similar results have been reported with cordycepin inhibiting mRNA synthesis (*11*). Moreover, the maximal FRP concentration produced by treatment with the iron chelator Desferal is achieved only if concomitant protein synthesis is allowed to occur (*4*). These results suggest that FRP ordinarily turns over in the presence of iron, which results in derepression of ferritin synthesis and degradation of Tf receptor mRNA.

To test this hypothesis, we determined the stability of newly synthesized FRP by first labeling rabbit cells for 2 hours in the absence of an iron source and then measuring radioactivity in FRP in the presence of added iron or heme (*14*). The immunoprecipitable label in FRP disappears as a result of treatment with heme (Fig. 1A). An early step in this degradative pathway appears to be the covalent linking of FRP to one or more other proteins. The major linked species migrates in SDS–polyacrylamide gel electrophoresis (PAGE) at about 200 kD. These intermediates are eventually degraded, with traces of presumptive degradation products sometimes visible at about 25, 40, and 70 kD. Formation of the linked species may be reversible after a brief exposure to heme (*15*).

Department of Biology, Washington University, St. Louis, MO 63130.

*To whom correspondence should be addressed.

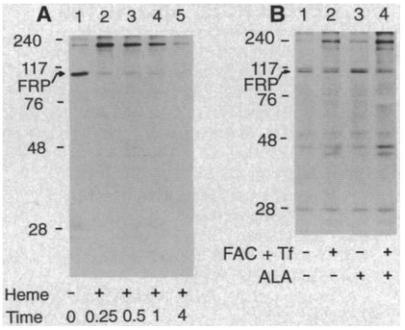

Fig. 1. Degradation of FRP that accompanies induction of ferritin synthesis by heme or iron. Rabbit RAB-9 cells were labeled with ^{35}S-methionine plus ^{35}S-cysteine for 2 hours (*14*). Washed twice with unlabeled media, cells were treated with (**A**) 50 μM heme in the presence of excess (1 mM) unlabeled methionine for the indicated times (hours) or with (**B**) excess (1 mM) unlabeled methionine for 6 hours in the presence, where indicated, of 100 μM FAC with Tf (0.2 mg/ml) or 2 mM ALA. Cells were then lysed, and labeled FRP was immune-precipitated with rat anti-rabbit FRP antibody and analyzed by SDS-PAGE and fluorography. Molecular size markers are indicated to the left in kilodaltons.

Treatment with iron can also stimulate FRP cross-linking and degradation (Fig. 1B and Table 1). These effects are increased by the presence of ALA (a committed precursor of porphyrin synthesis) but inhibited by succinylacetone (SA) and Desferal (both strong inhibitors of heme synthesis). These results suggest that the iron-porphyrin adduct, heme, is involved in the production of degradative effects. Neither Desferal nor SA blocks the effects of heme addition. None of these reagents significantly affects the stability of any other resolvable cellular protein (*15*).

As suggested by the loss of prelabeled FRP (Table 1, experiments 1 and 2), treatment of cells with iron or heme leads to a substantial reduction in the total FRP detectable by protein immunoblot analysis (*16*) (Table 1, experiment 3). However, the difference between the residual amounts of prelabeled FRP (7%) (Fig. 1A) and total FRP (37%) (Table 1, experiment 3) after a 4-hour treatment with 50 μM heme may be a result of the de novo synthesis of nonradioactive FRP in the presence of heme.

The increase in FRP produced by ALA treatment (Table 1, experiment 1) suggests that ALA, or a porphyrin product, might stabilize FRP by counteracting its degradation. This effect was inhibited by SA but not by Desferal (Table 1, experiment 2), which suggests that a precursor to heme, rather than heme itself, is responsible for FRP stabilization. In other experiments (*15*), we did not observe any effect of ALA or iron on the rate of FRP synthesis.

Whereas the conditions that potentiate FRP degradation also induce ferritin synthesis (*17*), the conditions that counteract FRP degradation inhibit ferritin synthesis induction. Desferal (200 μM), for example, completely inhibited ferritin synthesis induced by Tf, but had little or no effect on that induced by heme (*18*) (Fig. 2). Desferal's effects were similar to those noted for FRP stability. Similarly, SA inhibited ferritin synthesis induced by ferric ammonium citrate (FAC) or by Tf, but not that induced by heme (Table 2) (*19*). These results show that in the absence of significant porphyrin synthesis, iron by itself is a poor inducer of ferritin synthesis just as it is a poor stimulator of FRP degradation. The porphyrin precursors ALA and porphobilinogen (PBG) stimulated induction of ferritin synthesis at optimal iron concentrations (Table 2, experiment 2); however, at suboptimal iron concentrations (Table 2) or soon after addition of iron (3 to 4 hours) (*15*), these same precursors inhibited induction. These results reflect that at very low iron concentrations ALA stabilized FRP, but at higher iron concentrations it promoted FRP degradation (Table 1). Thus, a porphyrin intermediate may counteract the derepressive effect of heme by inhibiting FRP degradation.

Our results indicate that iron, probably acting through heme, can trigger the degradation of FRP: the resulting deficit in FRP causes derepression of ferritin and erythroid ALA-synthase mRNA translation and destabilization of Tf receptor mRNA. This process represents a novel mechanism for regulating gene expression. Although rapid degradation of regulatory factors is commonly seen in transcriptionally controlled systems (*20*), an analogous mechanism has not been previously observed at the translational level. A slight imbalance between the rates of FRP synthesis and degradation, such as might be effected by a slight rise in the intracellular heme concentration, could lead to the derepression of ferritin synthesis. This might explain why such large amounts of heme are needed to derepress ferritin synthesis in vitro, where FRP cross-linking (*21*) but not degradation occurs. Because the inductive effect of heme may be counteracted by a porphyrin precursor, the heme-porphyrin ratio, rather than heme per se, might govern the activity of FRP. This could explain why heme and heme analogs can induce the translation of erythroid ALA-synthase mRNA (*8*, *22*): action of this enzyme in the absence of a sufficient iron influx would lead to an excess of porphyrin precursors, which would stabilize FRP and shut down ALA-synthase production. A porphyrin precursor might act by binding to the heme site on FRP (*21*) without inactivating the protein or triggering its degradation; protoporphyrin IX, for example, does not inhibit FRP function in vitro (*9*).

In addition to serving as a substrate for heme synthesis, free iron may form an iron-sulfur center in FRP. A large number of amino acid residues in FRP are homologous to those at the iron-binding center of aconitase and to isopropylmalate isomerase

Table 1. Quantitation of the degradation of FRP that accompanies induction of ferritin synthesis in vivo (*14*). Rabbit RAB-9 cells were pulse-labeled with ^{35}S-methionine plus ^{35}S-cysteine for 2 hours. Excess unlabeled methionine was then added in the presence of 100 μM FAC plus Tf (0.2 mg/ml), 7.5 mM SA, 200 μM Desferal, or ALA or heme as indicated, for 6 hours (or for the times shown in experiment 3). In experiments 1 and 2, labeled FRP was then immune-precipitated and analyzed by SDS-PAGE, fluorography, and densitometry. In experiment 3, lysates were submitted to protein immunoblot analysis (*16*), followed by densitometric quantitation of FRP.

Addition	Relative radioactivity in FRP (% of control)
Experiment 1	
None	100
FAC + Tf	77
FAC + Tf + ALA (2 mM)	33
FAC + Tf + ALA (2 mM) + SA	99
ALA (2 mM)	125
SA + ALA (2 mM)	103
Heme (10 μM)	25
Heme (10 μM) + SA	19
Heme (20 μM)	16
Heme (20 μM) + SA	15
Heme (50 μM)	9
Heme (50 μM) + SA	8
Heme (50 μM) + Desferal	8
Heme (100 μM)	4
Heme (100 μM) + SA	4
Experiment 2	
None	100
FAC + Tf	71
FAC + Tf + ALA (0.5 mM)	68
FAC + Tf + ALA (2 mM)	58
FAC + Tf + ALA (8 mM)	51
FAC + Tf + Desferal	104
FAC + Tf + Desferal + ALA (0.5 mM)	128
FAC + Tf + Desferal + ALA (2 mM)	120
FAC + Tf + Desferal + ALA (8 mM)	131
FAC + Tf + SA + ALA (0.5 mM)	92
FAC + Tf + SA + ALA (2 mM)	92
FAC + Tf + SA + ALA (8 mM)	90
Experiment 3	
None	100
Heme (50 μM) (4 hours)	37
FAC + Tf (5 hours)	82
FAC + Tf + ALA (2 mM) (5 hours)	68
Heme (50 μM) (2 hours)	39
Heme (50 μM) (2 hours) then Desferal (6 hours)	79
Desferal (6 hours)	100

(*23*), and FRP has aconitase activity (*24*). The acquisition of iron by an Fe_3S_4 cluster in FRP to form an Fe_4S_4 cluster might result in inactivation of the protein and consequent derepression of ferritin synthesis (*23*). Although this mechanism is thought to be reversible, it is compatible with the essentially irreversible mechanism proposed here. However, the apo (lacking iron) form of the protein (*6*, *25*) can bind to an IRE; thus further experimentation is required to elucidate the precise roles of various forms of the iron-sulfur center for FRP activity. The heme and iron-sulfur centers may represent different ways of responding to iron excess and thus represent redundant control mechanisms (*1*).

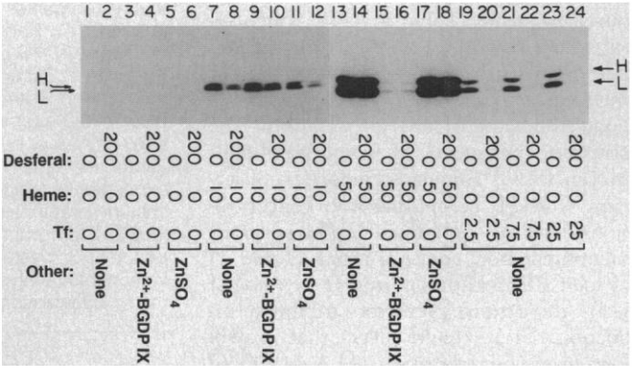

Fig. 2. Effect of Desferal on the induction of ferritin synthesis. Transformed mouse epithelial (C22) cells were grown to confluence for 2 days as described (*14*, *17*). Media were then supplemented with Desferal (Ciba-Geigy, Ardsley, New York), heme, or Tf at the concentrations indicated (micromolar). Where indicated, cells had been pretreated for 16 hours with 50 μM Zn^{2+}–BGDP IX, an inhibitor of heme oxygenase, or 50 μM $ZnSO_4$. After 4 hours, cells were pulse-labeled, washed, and lysed, and mouse ferritin was precipitated with anti-mouse ferritin serum raised in rabbits. The immune-precipitated mouse ferritin was then analyzed by SDS-PAGE and fluorography. H, heavy chain; L, light chain.

Table 2. Effects of SA, ALA, and PBG on the induction of ferritin synthesis. Mouse C22 cells (experiment 1) or rabbit RAB-9 cells (experiment 2) were treated with FAC, heme, Tf, SA, ALA, or PBG at the concentrations indicated (*17*). After 4 hours (experiment 1) or 11 hours (experiment 2), cells were pulse-labeled for 1 hour with ^{35}S-methionine plus ^{35}S-cysteine, and labeled ferritin was analyzed by immune precipitation, SDS-PAGE, and fluorography. Fluorograms were quantitated by densitometry. Control values (without iron) were subtracted from all values shown in experiment 1. ND, no ferritin synthesis was detected.

FAC (μM)	Heme (μM)	Tf (mg/ml)	Other additions (mM)	Relative radioactivity in	
				H-chain	L-chain
			Experiment 1		
0	10	0	None	3330	198
0	10	0	SA (2.5)	3433	140
0	10	0	SA (7.5)	2891	219
0	10	0	SA (15)	3065	231
100	0	0	None	2756	499
100	0	0	SA (2.5)	2454	243
100	0	0	SA (7.5)	547	34
100	0	0	SA (15)	299	ND
0	0	0.2	None	814	ND
0	0	0.2	SA (2.5)	975	ND
0	0	0.2	SA (7.5)	544	ND
0	0	0.2	SA (15)	299	ND
			Experiment 2		
0	0	0	None	160	6
0	0	0	ALA (1.0)	100	2
0	0	0.2	None	274	12
0	0	0.2	ALA (1.0)	134	4
10	0	0	None	222	10
10	0	0	ALA (1.0)	132	6
50	0	0	None	292	10
50	0	0	ALA (1.0)	346	26
100	0	0.2	None	2524	210
100	0	0.2	ALA (0.5)	5552	892
100	0	0.2	None	2674	170
100	0	0.2	PBG (1.0)	3094	234
100	0	0.2	PBG (10)	4078	523

REFERENCES AND NOTES

1. R. S. Eisenstein and H. N. Munro, *Enzyme* **44**, 42 (1991); E. C. Theil, *ibid.*, p. 68; J.-J. Lin, W. E. Walden, R. E. Thach, *ibid.*, p. 59.
2. J. B. Harford and R. D. Klausner, *ibid.*, p. 28.
3. B. Neupert, N. A. Thompson, C. Meyer, L. Kuhn, *Nucleic Acids Res.* **18**, 51 (1990).
4. E. W. Mullner *et al.*, *Cell* **58**, 373 (1989).
5. T. A. Rouault *et al.*, *Proc. Natl. Acad. Sci. U.S.A.* **86**, 5768 (1989); H. A. Barton *et al.*, *J. Biol. Chem.* **265**, 7000 (1990).
6. W. E. Walden, M. M. Patino, L. Gaffield, *J. Biol. Chem.* **264**, 13765 (1989).
7. T. A. Rouault *et al.*, *Proc. Natl. Acad. Sci. U.S.A.* **87**, 7958 (1990).
8. T. Dandekar *et al.*, *EMBO J.* **10**, 1903 (1991); T. C. Cox *et al.*, *ibid.*, p. 1891.
9. J.-J. Lin *et al.*, *Science* **247**, 74 (1990); J.-J. Lin, M. M. Patino, L. Gaffield, W. E. Walden, R. E. Thach, *Biochim. Biophys. Acta* **1050**, 146 (1990); G. S. Swenson *et al.*, *Biol. Metals* **4**, 48 (1991); J. H. Ward *et al.*, *J. Biol. Chem.* **259**, 13235 (1984); U. Muller-Eberhard *et al.*, *ibid.* **263**, 14753 (1988); M. L. Adams, I. Ostapiuk, J. A. Grasso, *Biochim. Biophys. Acta* **1012**, 243 (1989).
10. R. S. Eisenstein *et al.*, *Proc. Natl. Acad. Sci. U.S.A.* **88**, 688 (1991); T. Rouault, K. Rao, J. Harford, E. Mattia, R. D. Klausner, *J. Biol. Chem.* **260**, 14862 (1985); S. S. Bottomley, L. C. Wolfe, K. R. Bridges, *ibid.*, p. 6811.
11. J. Rogers and H. N. Munro, *Proc. Natl. Acad. Sci. U.S.A.* **84**, 2277 (1987).
12. S. Daniels-McQueen, L. S. Goessling, R. E. Thach, unpublished observations.
13. W. E. Walden *et al.*, *Gene* **61**, 317 (1987).
14. Two cell lines were used for most experiments: RAB-9, a normal rabbit skin fibroblast, and C22, a bovine papilloma virus–transformed mouse epithelial cell line (*26*). Several experiments were repeated with the nontransformed parental line of C22 (C127). All data were repeated more than once, except for the experiments with 10 mM and 100 mM heme (Table 1). No significant differences were observed among the three cell lines studied. For most experiments, cells were seeded at low density in Earle's minimal essential medium (MEM) supplemented with 2% fetal calf serum [and with nonessential amino acids (alanine, aspartate, glutamate, glycine, proline, and serine, all at 0.1 mM) and 1 mM sodium pyruvate for RAB-9 cells], and allowed to grow for 2 days (for C22 and C127 cells) or for 5 days (for RAB-9 cells) with refeeding after 3 days. For analysis of radiolabeled FRP, RAB-9 cells were labeled with ^{35}S-methionine plus ^{35}S-cysteine (^{35}S-Trans; ICN) for 2 hours in serum-free medium and then transferred to spent media that contained 1 mM unlabeled methionine and, where indicated, 100 μM FAC with Tf (0.2 mg/ml), 200 μM Desferal, ALA, PBG, SA, or heme at the indicated concentrations and times (Fig. 1 and Table 1). Residual radiolabeled FRP was then analyzed by immune precipitation of equal counts per minute of labeled lysate [pretreated with 1.1% SDS at 100°C for 5 min, then diluted fivefold with immune buffer that contained bovine serum albumin (13 mg/ml) and no SDS] with rat anti-FRP serum, SDS-PAGE, and fluorography, all as described (*13*, *26*, *27*).
15. L. S. Goessling, S. Daniels-McQueen, J.-J. Lin, R. E. Thach, unpublished observations.
16. J. Towbin, T. Staehelin, J. Gordon, *Proc. Natl. Acad. Sci. U.S.A.* **76**, 4350 (1979); W. N. Burnette, *Anal. Biochem.* **112**, 195 (1981); M. S. Blake *et al.*, *ibid.* **136**, 175 (1984).
17. Ferritin synthesis was induced by treatment of cells with heme, Tf, or FAC (Fig. 2 and Table 2). Where indicated in Fig. 2 or Table 2, ALA, SA, PBG, or Desferal was also present at the indicated concentrations. To inhibit heme oxygenase, we pretreated cells for 16 hours with 50 μM Zn^{2+}–bisglycol-deuteroporphyrin IX (Zn^{2+}–BGDP IX) or $ZnSO_4$ as a control. Newly synthesized proteins were labeled for 1 or 2 hours with ^{35}S-methionine plus ^{35}S-cysteine, cells were lysed, and equal counts per minute of labeled

lysate were immune-precipitated with antiferritin antibody and analyzed by SDS-PAGE and fluorography, all as described (*13, 26, 27*).
18. A slight inhibition of ferritin synthesis by Desferal was seen only at a low heme concentration (10 μM). However, this effect was prevented by preincubation with either Zn^{2+}–BGDP IX (Fig. 2) or Sn^{4+}–protoporphyrin IX (*15*), both potent inhibitors of heme oxygenase (which is normally responsible for rapid heme turnover) (*28*). This result suggests that at low heme concentrations, the effect of Desferal is a result of inhibition of the recycling of iron released by heme oxygenase action. By contrast, heme oxygenase inhibitors did not prevent the inhibition by Desferal of Tf-induced ferritin synthesis. Inhibition of heme oxygenase by Zn^{2+}–BGDP IX was so severe that addition of 50 μM heme to treated cells resulted in cell lysis (Fig. 2), which presumably resulted from an inability to detoxify such a high concentration of heme. Inhibition of heme oxygenase by metalloporphyrins was confirmed by direct measurement (N. Abraham).
19. The large amount of SA required to inhibit ferritin synthesis induced by FAC or Tf is consistent with other observations that suggest the existence of a large intracellular excess of ALA dehydratase (*29*). In our initial studies, 1.0 mM SA inhibited heme synthesis by greater than 98% when added 4 hours before the pulse labeling of heme with either ^{59}Fe- or ^{14}C-ALA. However, 1.0 mM SA had little effect on total protein synthesis, on ferritin synthesis in the presence or absence of inducers, or on cell growth rate. Cells grown for 5 days in 1.0 to 2.0 mM SA as described (*14*) produced cell numbers and protein mass indistinguishable from cells grown in control media. Cells grown in 2.5 to 5.0 mM SA grew 77% as fast as control cells, as indicated by the same criteria. These results suggest that only a small fraction of the cell's ALA-dehydratase activity is sufficient to supply all normal heme requirements. This result is also consistent with our finding that protein synthesis is inhibited only 4% and 24% by 7.5 mM and 15 mM SA, respectively (*15*).
20. J. W. Roberts and C. W. Roberts, *Nature* **290**, 422 (1981); M. Hochstrasser, J. J. Ellison, V. Chan, A. Varshavsky, *Proc. Natl. Acad. Sci. U.S.A.* **88**, 4606 (1991); A. Ciechanover *et al.*, *ibid.*, p. 139; M. Scheffner *et al.*, *Cell* **63**, 1129 (1990).
21. J.-J. Lin *et al.*, *Proc. Natl. Acad. Sci. U.S.A.* **88**, 6068 (1991).
22. C. S. Chang and S. Sassa, *J. Biol. Chem.* **257**, 3650 (1982).
23. T. A. Rouault *et al.*, *Cell* **64**, 881 (1991); M. W. Hentze and P. Argos, *Nucleic Acids Res.* **19**, 1739 (1991).
24. S. Kaptain *et al.*, *Proc. Natl. Acad. Sci. U.S.A.* **88**, 10109 (1991).
25. L. Zheng and H. Zalkin, personal communication.
26. T. G. Lawson *et al.*, *J. Virol.* **63**, 5013 (1989).
27. P. H. Brown *et al.*, *J. Biol. Chem.* **264**, 13383 (1989).
28. R. J. Chernik *et al.*, *Hepatology* **10**, 359 (1989).
29. F. Iwasa, S. Sassa, A. Kappas, *Biochem. J.* **262**, 807 (1989).
30. This work was supported by grants from NSF (DMB 88-18106) and NIH (AI 20484). We are grateful to W. E. Walden for donating purified rabbit FRP and mouse anti-rabbit FRP serum for comparison and for useful discussions.

22 November 1991; accepted 16 March 1992

Occurrence of Sialic Acids in *Drosophila melanogaster*

Jürgen Roth,* Andreas Kempf, Gerd Reuter, Roland Schauer, Walter J. Gehring

Sialylated oligosaccharides, which are cell type–specific and developmentally regulated, have been implicated in a variety of complex biological events. Their broad functional importance is reflected by their presence in a wide variety of phyla extending from *Echinodermata* through higher vertebrates. Here, sialic acids are detected throughout development in an insect, *Drosophila*. Homopolymers of α 2,8-linked sialic acid, polysialic acid, are developmentally regulated and only expressed during early *Drosophila* development.

Sialic acids comprise a large family of closely related derivatives of *N*-acetylneuraminic acid and *N*-glycolylneuraminic acid (*1*). Terminal glycosylation sequences, in particular sialylated oligosaccharides that are cell type–specific and developmentally regulated, have been implicated in a variety of complex biological events (*2*). The expression of various specific sialyltransferases is the basis for the synthesis of such glycosylation sequences (*3*). Sialic acids can be found in a variety of chemical linkages, including linkage to different penultimate sugars of a glycosylation sequence. Specific sequences expressed in one context may be critical for biological recognition but may have no function in another context (*2*) as shown in studies of sialic acids during organogenesis (*4*), cell differentiation (*5*), endothelial cell leukocyte adhesion molecule (ELAM-1)–mediated cell adhesion (*6*), interaction of viruses and certain pathogenic bacteria with their host cells (*7*), and tumor cell invasiveness (*8*). Sialic acids are found in the *Echinodermata* and in most chordates

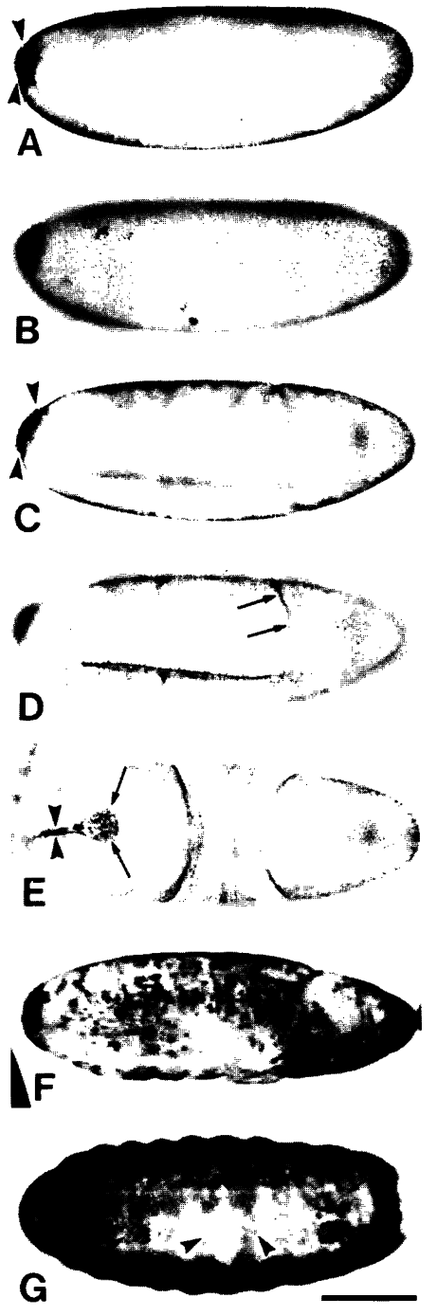

Fig. 1. Cytochemical detection of sialic acid in *Drosophila* embryos with use of the *Limax flavus* lectin (*11*). (**A**) Whole mount of a blastoderm stage embryo (*20*) showing intensely stained pole cells (arrowheads) and stained blastoderm cells. (**B**) Same embryo as in (A) at another plane of focus to demonstrate the honeycomb pattern of lectin staining on blastoderm cells. (**C** and **D**) Early gastrulation stage embryo. Staining of pole cells [arrowheads in (C)] and blastoderm cells is evident, along with additional labeling along the ventral [arrowheads in (D)] and cephalic [arrows in (D)] furrows. (**E**) Rapid phase of germ band elongation. Dorsal view of an embryo that exhibits staining of the ventral furrow (arrowheads) and the invaginating pole cells (arrows) as well as the honeycomb staining pattern. (**F**) Embryo with fully extended germ band. Small groups of cells at both sides of the ventral furrow are more intensely stained than neighboring cells. (**G**) Embryo after germ band shortening and during dorsal closure exhibits staining in the ventral nervous system (arrowheads) and the brain ganglia (arrows). In all photographs embryos are oriented with the anterior end to the right. Scale bar = 0.1 mm.